European Journal of Pharmaceutics and Biopharmaceutics 71 (2009) 395–401

Contents lists available at ScienceDirect

European Journal of Pharmaceutics and Biopharmaceutics

journal homepage: www.elsevier.com/locate/ejpb

Research paper

On the physical interpretation of the initial bending of a Shapiro–Konopicky–Heckel compression profile

Ingvild Klevan [a,*], Josefina Nordström [b,*], Annette Bauer-Brandl [a], Göran Alderborn [b]

[a] Institute of Pharmacy, University of Tromsø, Tromsø, Norway
[b] Department of Pharmacy, Uppsala University, Uppsala, Sweden

ARTICLE INFO

Article history:
Received 30 May 2008
Accepted in revised form 30 September 2008
Available online 7 October 2008

Keywords:
Powder compression
Heckel
Shapiro
Fragmentation
Powder compression classification system
Powder technology

ABSTRACT

The relationship between the natural logarithm of the tablet porosity and the applied pressure is used to describe the compression behavior of a powder. Such a relationship, here referred to as a Shapiro–Konopicky–Heckel (*SKH*) profile, is usually divided into three regions, of which the first often is non-linear. The objective of this work was to address the question of the mechanisms controlling the compression and the bending of the first region of a *SKH* profile for dense particles. In this paper, the first region was described by the Shapiro General Compression Equation, from which a compression parameter was derived as a measure of the bending. The results indicate that for powders undergoing significant particle rearrangement at low applied pressures, the particle rearrangement is the major cause for the initial bending of the *SKH* profile. For powders showing limited particle rearrangement, the initial bending is mainly caused by the change in particle diameter due to particle fragmentation. It is concluded that the evaluation of the first region of a *SKH* profile in terms of bending may be used to assess particle fragmentation. The *SKH* profile could hence be a useful tool to describe powder compression behavior in terms of particle fragmentation and particle deformation from one single compression analysis.

1. Introduction

The use of the natural logarithm of the tablet porosity or tablet relative density as a function of the applied pressure has evolved as a common means to describe the compression of a powder in different fields of powder technology. Shapiro [1] and Konopicky [2] published powder compression data using this approach, but in the pharmaceutical field the type of profile is most commonly referred to as the Heckel equation [3], and the natural logarithm of the inverted tablet porosity is sometimes denoted the Heckel number [4]. In this paper, this relationship is hereafter referred to as the *SKH* (Shapiro–Konopicky–Heckel) profile. A common approach of interpreting a *SKH* profile is that the profile can be divided into three regions [5,6]. Firstly, an initial non-linear part with a falling derivative (i.e. a concave compression profile, here denoted region I), followed by a linear part in which the data obey the expression (region II) and finally, a second non-linear part with an increasing derivative (i.e. a convex compression profile, here denoted region III). The physical explanation for these three regions of the profile is normally provided in terms of rate controlling compression mechanisms that vary between the different regions.

For region II, it is argued that particle deformation is the controlling mechanism, either reversible or permanent [7], and for region III it is proposed that elastic deformation of the whole tablet controls the compression process [5]. For region I finally, Denny [8] has summarized the proposed explanations for the deviation of linearity often observed for different types of particulate solids. Excluding one of the explanations concerning the problem of constructing a *SKH* profile for porous, secondary particles (i.e. agglomerates) [9–11], two main reasons are discussed in the literature. The first, proposed by Shapiro and Heckel, is that the curvature is due to particle rearrangement (powder flow) during compression. This explanation seems to be preferred in the literature for a spectrum of materials exhibiting ductile to brittle behavior [5,7]. The other explanation is that particles fragment during compression and that this fragmentation causes a gradual change in the derivative of the curve until fragmentation ceases to occur. This explanation was suggested by Duberg and Nyström [12] and it has also been used in the modeling of a Heckel profile of a fragmenting (brittle) particulate solid [13].

The conception that fragmentation and deformation are the two processes controlling the compression in region I and II, respectively, is interesting since it offers the opportunity to derive indicators of both the fragmentation propensity and the deformation propensity of particles in a single compression test. The Shapiro

* Corresponding authors. Institute of Pharmacy, University of Tromsø, N-9037 Tromsø, Norway. Tel.: +46 (0) 18 4714372 (I. Klevan); Department of Pharmacy, Uppsala University, Box 580, SE-751 23 Uppsala, Sweden. Tel.: +46 (0) 18 4714550 (J. Nordström).
E-mail addresses: ingvild.klevan@farmasi.uit.no (I. Klevan), josefina.nordstrom@farmaci.uu.se (J. Nordström).

0939-6411/$ - see front matter © 2008 Elsevier B.V. All rights reserved.
doi:10.1016/j.ejpb.2008.09.014

General Compaction Equation (GCE) [14] was derived as a means to describe region I and II in one single equation, and consists of two parts that describe the different regions, respectively. Two compression parameters can thus be derived that hypothetically can be used as indicators of the compression process of the respective regions. However, in order to physically interpret such parameters, the question of the physical significance of the bending of region I of the *SKH* profile, i.e. if it is due to particle rearrangement or particle fragmentation, remains to be resolved. In a previous paper [15], a classification of powders into different groups based on an index describing the extent of particle rearrangement during compression was proposed as a means to facilitate the physical interpretation of global compression parameters. The objective of this present work was to explore this further by addressing the question of the physical interpretation of the bending of region I of the *SKH* compression profile.

2. Materials and methods

2.1. Model materials

The four different model materials used here were the same as in a previous study [15], namely, sodium chloride (apparent particle density = 2.152 g/cm^3, crystalline, Fluka, Steinheim, Germany), sodium bicarbonate (apparent particle density = 2.216 g/cm^3, crystalline, Fluka, Steinheim, Germany), lactose (apparent particle density = 1.540 g/cm^3, crystalline α-monohydrate, Pharmatose®, DMV International, Veghel, The Netherlands) and sucrose (apparent particle density = 1.586 g/cm^3, crystalline, Fluka, Steinheim, Germany).

For each model material, four powders of different fineness were prepared, hereafter denoted fraction 1, 2, 3 and 4. The two coarsest size fractions (250–300 μm and 125–180 μm) were obtained by dry sieving (Retsch, type RV, Haan, Germany). Fraction 3 was prepared by milling the raw material in an electrical mortar grinder (Retsch, Grindomat KM1, Haan, Germany) followed by particle separation in an air classifier (Alpine 100MZR, Alpine AG, Augsburg, Germany) and finally, fraction 4 was obtained by milling the raw material in a pin disk mill (Alpine 63C Contraplex Labormühle, Alpine AG, Augsburg, Germany). The particle sizes were examined visually by optical light microscopy (model Vanox, Olympus, Tokyo, Japan). All powders were conditioned at a constant relative humidity (∼40%) and room temperature (∼20 °C) for at least 7 days before any further experiments, even though it has earlier been reported [16] that for non-hygroscopic materials, a variation in relative humidity had a negligible effect on the compression behavior of a powder until condensed water appeared.

2.2. Powder characterization

The powders were characterized with respect to their bulk density (ρ_{bulk}) and their volume specific surface area (S_0). The procedures used are described in greater detail and the results obtained are reported in the previous paper [15], but are used in this work to determine the fragmentation tendency and a compression parameter of the powders (see below). The volume specific surface areas and bulk porosities are therefore given in Table 1.

The bulk density was measured by gentle pouring the powder samples (3.5–10.3 g) into a graduated 10 ml cylinder (10 mm in diameter) and the volume of the powder bed was determined visually (n = 3).

The volume specific surface area of the two coarsest size fractions was measured using a steady-state air permeability apparatus and calculated with the Kozeny–Carman equation [17,18]. The powder was poured into a glass cylinder (11.47 mm in diameter) and weighed (1.2–3.7 g) and the height of the powder bed was measured (Mitutoyo Digimatic, ID-C, Tokyo, Japan) before the cylinder was mounted on the steady-state air permeability apparatus. The pressure in the closed system was measured at five different percentage rates of airflow and three recordings of flow rate and pressure were done for each percentage. The experiment was repeated three times per powder. The volume specific surface area of the two finest size fractions was determined using a transient (Blaine) air permeability apparatus [17]. For these powders, S_0 was calculated using a slip flow corrected Kozeny–Carman equation [19] and the reported results are the mean of two separate experiments with three recordings of flow time for each experiment.

Table 1
Permeametry results and compression parameters derived from linear regression analysis of *in-die SKH*-profiles in the pressure interval 50–150 MPa. All values are mean values (n = 3) and the relative standard deviations are denoted in parentheses.

		S_0[a] (cm^2/cm^3)	S_T[b] (cm^{-1})	Δd[c] (μm)	P_y[d] (MPa)	A[e] (–)
Sodium chloride	1	313 (0.01)	349 (0.20)	33	69.9 (0.08)	0.99 (0.04)
	2	623 (0.06)	826 (0.04)	49	86.8 (0.03)	1 (0.01)
	3	2559 (0.03)	2986 (0.07)	6	94.9 (0.01)	0.81 (0.01)
	4	3115 (0.04)	4066 (0.05)	8	137 (0.26)	0.94 (0.03)
Sucrose	1	406 (0.06)	2940 (–)*	213*	161 (0.01)	1.28 (0.01)
	2	676 (0.03)	2550 (0.05)	109	154 (0.01)	1.307 (0.01)
	3	1393 (0.05)	2667 (0.02)	34	143 (0.03)	1.18 (0.03)
	4	2945 (0.03)	6417 (0.05)	18	196 (0.12)	1.16 (0.09)
Sodium bicarbonate	1	454 (0.03)	4567 (0.05)	198	164 (0.01)	1.28 (0.01)
	2	756 (0.01)	2165 (0.05)	86	166 (0.01)	1.19 (0.01)
	3	1968 (0.01)	3316 (0.24)	21	184 (0.01)	1.02 (0.01)
	4	3619 (0.06)	5666 (0.08)	10	280 (0.11)	1.01 (0.02)
Lactose	1	330 (0.21)	2037 (0.01)	254	124 (0.01)	1.33 (0.01)
	2	655 (0.04)	2875 (0.02)	118	126 (0.01)	1.28 (0.01)
	3	1033 (0.05)	3306 (0.03)	67	130 (0.01)	1.18 (0.01)
	4	3040 (0.01)	14046 (0.07)	26	238 (0.27)	1.25 (0.08)

[1] 250–300 μm; [2] 125–180 μm; [3] Milled and air jet classified; [4] Milled.
[a] The volume specific surface area S_0 of the powder samples determined on a steady-state air permeability apparatus.
[b] Volume specific tablet surface area at 50 MPa (cm^{-1}), (sucrose 250–300 μm, n = 1).
[c] Estimated change in particle size (μm).
[d] Mean yield pressure derived from the Heckel equation (MPa).
[e] Intercept from linear regression analysis of a Heckel profile.
* Single data point.

The S_0 obtained by the permeability experiments was transformed into an estimate of the original particle size (d_{S0}) as the ratio between a surface to volume shape factor and S_0. Generally, a constant surface to volume shape factor of 10 was used in the calculation [20].

2.3. Characterization of compressed powders

An instrumented single-punch press (Korsch EK0, Berlin, Germany), equipped with 11.3 mm diameter flat-faced punches, was operated manually by hand to produce five tablets from each material and size fraction (with the exception of the coarsest sucrose powder) at an applied pressure of 50 MPa according to a compaction and measurement procedure described elsewhere [19]. An amount of ~500 mg powder was poured by hand into a special die, built to fit a transient (a Blaine instrument) permeameter. The weight (analytical balance) and the height of the tablets (Mitutoyo Digimatic, ID-C, Tokyo, Japan) were measured and the die was thereafter immediately connected to the permeameter, and the time for a predetermined volume of air to pass through the tablet was determined. The volume specific surface area of the tablet (S_T) was finally calculated with a slip flow corrected Kozeny–Carman equation [19].

As an estimate of the change in particle diameter (Δd) that occurred during compression up to an applied pressure of 50 MPa, the difference in the reciprocals of the volume specific surface area of the original powder (S_0) and of the tablet (S_T) was calculated (using a constant surface to volume shape factor of 10 in the calculation [20]), i.e.

$$\Delta d = 10 * \left(\frac{1}{S_0} - \frac{1}{S_T}\right) \quad (1)$$

2.4. Powder compression

Confined compression of the powders was performed using a materials testing machine (Zwick Z100, Zwick/Roell Zwick GmbH & Co. KG, Ulm, Germany), also equipped with 11.3 mm diameter flat-faced punches. The lower punch was stationary during the compaction and the upper punch moved at a speed of 1 mm/min. All powder compression data were corrected for the determined elastic deformation of the punches according to a procedure described in a previous work [21]. The die and punch faces were lubricated with a 1% magnesium stearate suspension in ethanol prior to the compression. The material for each tablet was weighed (~500 mg) and poured by hand into the die. Three tablets from each material and size fraction were produced at a maximum pressure of 500 MPa.

2.5. Compression parameters

As an indicator of the powder compression process in region I of a compression profile, the Shapiro compression parameter, here denoted f, was derived from the Shapiro GCE [14], i.e.

$$\ln(E) = \ln E_0 - kP - fP^{0.5} \quad (2)$$

where E is the porosity of the powder bed, E_0 the initial porosity of the powder bed, P the applied compression pressure and k and f constants. The Shapiro compression parameter f is an indication of the degree of curvature of region I of the compression profile, and the compression parameter k is an indication of the linear part of the compression profile. In the calculation of the parameter f, curve-fitting of the experimental data was done by the least squares method in the same pressure range as was used in the estimation of the change in particle diameter (Δd) that occurred during compression, i.e. a pressure range up to an applied pressure of 50 MPa.

It has earlier been discussed [15,22,23] that the first value of the powder bed porosity (E_0) in the die and the corresponding pressure may affect the value of a derived compression parameter, i.e. the choice of lowest compression pressure in the pressure range of region I may affect the derived Shapiro parameter f. The Shapiro parameter f was therefore calculated using three different initial compression pressures of region I, i.e. firstly, 0 MPa (the bulk porosity corresponding to zero pressure was transformed from the measured bulk density, i.e. E_{0BD}) ($R^2 > 0.996$ for the coarser powders and $R^2 > 0.928$ for the finest powder), secondly, a fixed starting pressure of ~0.3 MPa ($R^2 > 0.995$ for the coarser powders and $R^2 > 0.974$ for the finest powder), and finally, a fixed starting pressure of ~1 MPa ($R^2 > 0.999$ for all powders).

As an indicator of the powder compression process in region II of a compression profile, the compression parameter often referred to as the Heckel parameter or the yield pressure of the particles was derived from the relationship between the Heckel number and the compression pressure [3]:

$$\ln\frac{1}{E} = kP + A \quad (3)$$

where E is the porosity of the powder bed, P the applied compression pressure, k and A constants and $\ln(1/E)$ is the Heckel number. The slope (k) was calculated by linear regression in the pressure range from 50 MPa up to 150 MPa, R^2-values >0.994 for all materials, i.e. a constant pressure range for region II was used for all powders. The reported yield pressures, P_y, are the reciprocal of the slope k.

3. Results and discussion

3.1. Compression profiles and estimation of particle fragmentation and plastic deformation

The model materials were chosen in such a way that they represent powders of different mechanical and compression properties, according to earlier experiences [6,24,25]. Sucrose and lactose are considered to be moderately hard materials and show marked fragmentation and limited deformation during compression. Sodium chloride can be described as a moderately soft plastic material that shows limited fragmentation but a high degree of deformation during compression. Sodium bicarbonate is also considered to be a moderately hard material that shows limited deformation during compression but also limited particle fragmentation. The preparation of different particle size fractions of each material was done to further affect the compression behavior of the powders in terms of the degree of particle rearrangement, particle deformation and particle fragmentation that are expressed during compression. As descriptors of particle deformation and particle fragmentation, the Heckel parameter k and the change in tablet surface area with compression pressure are used in this study.

In Fig. 1, the *SKH* compression profiles are shown for all powders investigated in this study. For some of the lactose and sodium chloride powders, negative tablet porosities were obtained at high compression pressures and thus, no compression curves were drawn over a pressure threshold of about 375–425 MPa and 230–350 MPa for these powders. The reason for negative porosities has been discussed in the literature, and one explanation concerns changes of the particle density at high pressures associated with particle elastic deformation [5,26]. All other powder compression curves were drawn up to a pressure of 500 MPa.

The overall shape of the compression profiles depended both on the material and on the original particle size. At low pressures, all powders showed curved profiles (Fig. 2) and with increasing

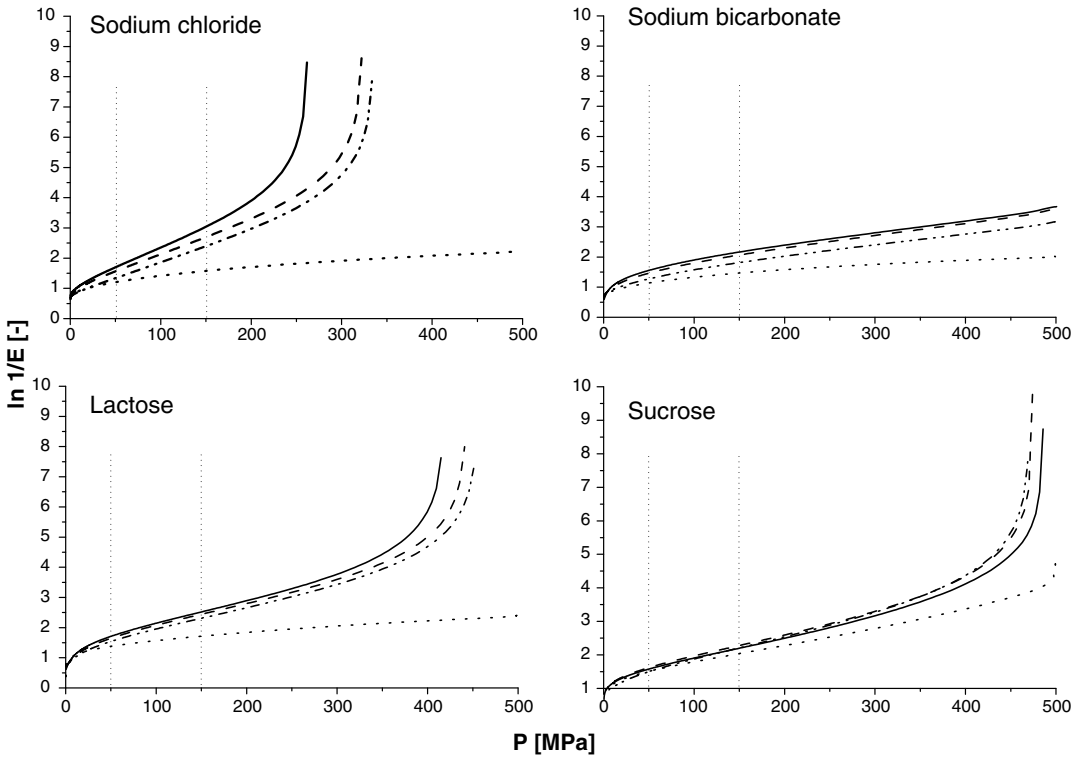

Fig. 1. Shapiro–Konopicky–Heckel compression profiles for all materials and size fractions in the pressure range 0–500 MPa. The dotted vertical lines indicate the boundaries between the three different regions of the compression profiles. The four powder finesses are distinguished as follows: 250–300 μm (—), 125–180 μm (– –), ~75 μm (– · · –) and <50 μm (·····).

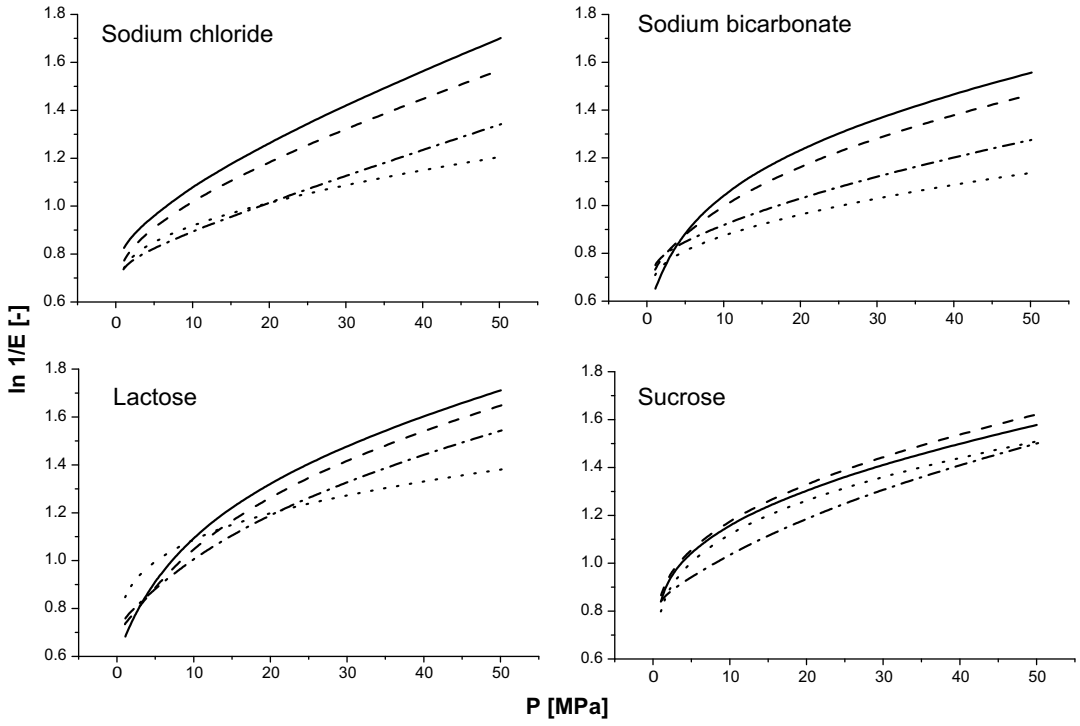

Fig. 2. Shapiro–Konopicky–Heckel compression profiles for all materials and size fractions in the pressure range 0–50 MPa (detail of Fig. 1). The four powder finesses are distinguished as follows: 250–300 μm (—), 125–180 μm (– –), ~75 μm (– · · –) and <50 μm (·····).

compression pressure, all powders showed a nearly linear compression profile. Thus, all powders expressed a compression behavior associated with region I and II. For fraction 1–3 of three of the materials (sodium chloride, lactose and sucrose), a clear bending also of the upper part of the *SKH*-profiles was obtained, which is a behavior associated with region III. All the finest pow-

ders (fraction 4) and all sodium bicarbonate powders showed limited bending at high pressures, i.e. only some of the powders expressed all three compression regions in the pressure range used in this study. As can be visually judged (Figs. 1 and 2), the compression pressures at which the transitions between the different regions of the compression profile occurred varied between the powders. Nevertheless, in order to compare the compression properties of the powders in a systematic but simple way in region I and II, fixed pressure ranges were used to define these regions. The transition pressure between region I and II was set to 50 MPa and the pressure range for region II was set to 50–150 MPa. These pressure levels were chosen in accordance with the ones previously used in the literature [5,27] and are indicated in Fig. 1 by dotted vertical lines.

To assess the degree of fragmentation of particles expressed during compression, the relationship between the permeametry surface area of tablets and the compaction pressure was studied [19,28]. As a means to indicate the degree of particle fragmentation that occurred in region I, the surface area of the original powders (S_0) as well as the surface area of tablets (S_T) formed at 50 MPa were determined and compared. Both the difference in surface area and an estimate of the difference in mean particle size (Δd) between powders and tablets were used in this comparison (Table 1). Sodium chloride showed in relative terms a small change in surface area and particle size with applied pressure, supporting that particles of sodium chloride showed limited fragmentation during compression. The data indicate further that lactose was most prone to fragment during compression while sucrose and sodium bicarbonate showed an intermediate behavior with a tendency for sucrose to be more prone to fragment. Thus, the measurements of the surface area of the powder and the tablets prepared at an applied pressure of 50 MPa indicate that the materials could be rank-ordered with respect to their fragmentation tendency in the following way: sodium chloride < sodium bicarbonate < sucrose < lactose. Regarding the effect of original volume specific surface area of the powders, the general trend was that an increased original powder surface area corresponded to a larger increase in surface area during compression, which is consistent with earlier observations [24]. An exception was, however, sodium bicarbonate for which the coarsest fraction showed a relatively large increase in surface area during compression. Regarding the change in estimated particle size that occurred during compression, there was a trend that a decreased original particle size corresponded to a smaller change in particle size during compression, ranging from an estimated change in particle size from ~250 μm to ~6 μm.

The Heckel parameter, often referred to as the yield pressure P_y, is a common means to derive an indication of the plasticity of particles. The compression profiles (Fig. 1) were generally linear in region II (see Section 2) and the calculated yield pressure values are given in Table 1. In general terms, the derived values of the yield pressure indicate that the materials could be rank-ordered in terms of their plasticity in the following way: sodium chloride > lactose > sucrose > sodium bicarbonate. For the respective material, the original powder surface area had a limited effect on the P_y values for fraction 1–3 powders without any consistent trend. However, for the respective material the highest P_y values were obtained for fraction 4 powders. Thus, the original particle size had a relatively limited effect on particle plasticity until a low particle size was reached for which the plasticity was markedly reduced.

In summary, the model powders used gave a series of shapes of the *SKH* profile dependent on the compression properties of the powders. All powders expressed region I and II of the profile and showed different combinations of particle plasticity and particle fragmentation tendency.

3.2. Physical interpretation of the bending of region I

The objective of this paper was to address the question of the physical interpretation of the bending of region I of the *SKH* compression profile, applicable to the compression of dense particles (Fig. 2). In order to derive a measure of this bending, a compression parameter, here denoted *f*, was calculated by the use of the Shapiro GCE (Eq. (3)) (Table 2). Visual examination of the compression profiles in region I (Fig. 2) indicates that the finest powders (fraction 4) generally showed the highest rate of initial compression, and the values of the *f* parameter were for the finest powders consequently strongly dependent on the value of the initial powder bed porosity (E_0). For the coarser powders, a much smaller influence of the initial porosity was obtained. As discussed earlier [15], a high initial compressibility due to the application of very low pressures is most likely a result of particle rearrangement, and it is concluded that only the finest powders showed significant particle rearrangement during compression. Visual examination of the compression profiles in region I indicates further that the finest powders (fraction 4) showed the sharpest bending of the profile. Consequently, for the set of values of the *f* parameter based on bulk porosity measurements (i.e. the f_1 parameter), the finest powders showed generally the highest f_1 values. It is therefore concluded that particle rearrangement is a process of importance for the bending of the *SKH* profile in region I. In the previous investigation [15], it was also suggested that the product (*ab*) of the Kawakita [29] compression parameters *a* and *b* could be used as an indication of the incidence of particle rearrangement during compression. In the present study, no general relationship between this index (*ab*) and the f_1 parameter was, however, obtained ($R^2 = 0.4129$, results not shown). Thus, particle rearrangement is not the only process affecting the shape of the compression profile (and hence the f_1 parameter) of region I.

When comparing the different materials, the powders of sodium chloride generally showed the least pronounced curvature of region I (Fig. 2). For these powders, the bending occurred primarily at low pressures ($P < 5$ MPa), and the profile tended to become linear already within the chosen pressure range of region I.

Table 2
Compression parameter *f* from the Shapiro GCE derived in three different pressure intervals. All values are mean values ($n = 3$) and the relative standard deviations are given in parentheses.

		f_1[a] (–)	f_2[b] (–)	f_3[c] (–)
Sodium chloride	1	0.09 (0.01)	0.09 (0.01)	0.09 (0.01)
	2	0.10 (0.03)	0.10 (0.01)	0.09 (0.01)
	3	0.04 (0.03)	0.04 (0.03)	0.04 (0.01)
	4	0.16 (0.69)	0.18 (0.05)	0.10 (0.07)
Sucrose	1	0.14 (0.003)	0.17 (0.01)	0.16 (0.005)
	2	0.17 (0.02)	0.16 (0.02)	0.15 (0.01)
	3	0.09 (0.20)	0.09 (0.21)	0.09 (0.24)
	4	0.35 (0.15)	0.18 (0.09)	0.15 (0.08)
Sodium bicarbonate	1	0.23 (0.02)	0.22 (0.02)	0.22 (0.02)
	2	0.13 (0.01)	0.13 (0.01)	0.13 (0.01)
	3	0.08 (0.003)	0.08 (0.003)	0.06 (0.01)
	4	0.21 (0.04)	0.09 (0.03)	0.08 (0.05)
Lactose	1	0.22 (0.01)	0.22 (0.01)	0.23 (0.01)
	2	0.16 (0.01)	0.16 (0.01)	0.17 (0.01)
	3	0.11 (0.005)	0.11 (0.004)	0.12 (0.01)
	4	0.33 (0.06)	0.14 (0.09)	0.13 (0.10)

[1] 250–300 μm.
[2] 125–180 μm.
[3] Milled and air jet classified.
[4] Milled.
[a] *SKH*-parameter *f* estimated in the range ($\ln E_{0\ BD}$–50) MPa.
[b] *SKH*-parameter *f* estimated in the range (0.3–50) MPa.
[c] *SKH*-parameter *f* estimated in the range (1–50) MPa.

The other materials showed a curvature extending over a larger range of pressures. Accordingly, the sodium chloride powders showed generally the lowest values of the f_1 parameter while lactose, the most fragmenting material, showed the highest values (Table 2). Since the bending of the compression profile in region I generally is consistent with the ranking of the fragmentation tendency of the materials (see above), it is concluded that particle fragmentation also is a process of importance for the initial bending of the *SKH* profile.

Concerning the effect of original powder surface area, the f_1 parameter tended to reduce with an increase in original powder surface area for fractions 1–3 (Table 2). This trend was broken with markedly increased values of the f_1 parameter for fraction 4, as discussed above. For the powders expressing limited particle rearrangement during compression, i.e. fractions 1–3 of all materials, the relationship between the f_1 parameter and the change in particle size during compaction (Δd) is presented in Fig. 3. It seems that all fractions followed a single non-linear relationship. It is thus concluded that for powders without significant initial particle rearrangement, the change in particle diameter due to particle fragmentation controls the bending in region I of an *SKH* profile.

The importance of particle fragmentation for the bending of the compression profile may be explained in two ways: firstly, the fracturing of a particle into smaller units may result in a rearrangement of the formed particles, i.e. a secondary particle rearrangement. Such a rearrangement may facilitate compression at low applied pressures. Secondly, the reduction in particle diameter due to particle fragmentation will progressively increase the hardness (reduce the plasticity) of the particles, corresponding to an increased yield pressure [24]. The resistance towards compression will consequently be controlled by a drifting yield pressure until particle fragmentation ceases to occur, i.e. a brittle to ductile transition [30]. From this point on, the hardness will be approximately constant and the rate of compression will obey the *SKH* model, i.e. the *SKH* profile will become linear.

Depending on the effect of original particle size on the shape of a *SKH* profile, a classification of such profiles has been proposed in the literature [31]. Based on the results presented in this paper, a new categorization of *SKH*-profiles into three types, dependent on the bending of the profile in region I with associated mechanistic explanation, is proposed (Fig. 4). The first category, denoted Type 1, is characterized by a sharp bending of region I due to significant particle rearrangement in combination with particle fragmentation. The second category, denoted Type 2, is characterized

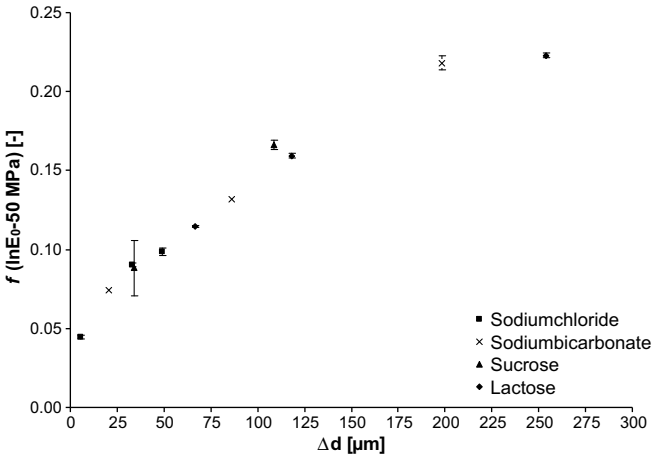

Fig. 3. The relationship between the estimated change in particle size, Δd, and the compression parameter f from the Shapiro General Compaction Equation shown for the three coarsest size fractions of the model materials. Mean and standard deviation, $n = 3$.

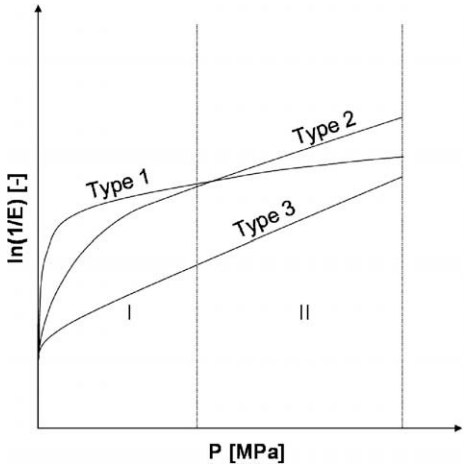

Fig. 4. A schematic illustration of the different types of Shapiro–Konopicky–Heckel profiles in region I and region II. Type 1 represents powders that undergoes initial particle rearrangement to a high extent, Type 2 represents powder that fragments during compression and finally, Type 3 represent plastic deforming powders with no significant initial particle rearrangement.

by a smoother and more extended bending of region I due to significant particle fragmentation without primary particle rearrangement. The third category, denoted Type 3, is characterized by a nearly linear region I due to limited particle rearrangement and limited fragmentation. For all three types, region II is approximately linear with particle deformation as rate controlling compression mechanism and a region III, associated with elastic deformation of the stiff tablet formed in the die, may appear dependent on the range of compression pressures used.

4. Conclusions

The question of the physical interpretation of the bending of region I of an *SKH* compression profile, applicable to the compression of dense particles at a slow and constant punch velocity, was addressed in this paper. The results indicate that for fine powders undergoing significant particle rearrangement at low applied pressures, particle rearrangement is the main cause for the initial bending of the *SKH* profile. For powders that show only limited initial particle rearrangement, the change in particle diameter due to particle fragmentation controls the initial bending of the *SKH* profile. A powder showing limited rearrangement and fragmentation will display a linear type of profile in region I. It is concluded that the evaluation of region I in a *SKH* compression profile in terms of the bending may be used as a means to assess particle fragmentation. The profile may therefore be a useful tool to describe powder compression behavior in terms of particle fragmentation and particle deformation from one single compression analysis. It is finally concluded that *SKH*-profiles can be categorized into three types dependent on the bending of the profile in region I with associated mechanistic explanation.

Acknowledgements

This study is part of a research program in Pharmaceutical Materials Science at Uppsala University, and financial support from the Vice chancellor of Uppsala University is gratefully acknowledged.

References

[1] I. Shapiro, PhD Thesis, University of Minnesota, 1944.
[2] K. Konopicky, Radex Rundsch (1948) 141.
[3] R.W. Heckel, Density–pressure relationships in powder compaction, Trans Metallurgy Society AIME 221 (1961) 671–675.

[4] J. Berggren et al., Compression behaviour and tablet-forming ability of spray-dried amorphous composite particles, European Journal of Pharmaceutical Sciences 22 (2–3) (2004) 191–200.
[5] C. Sun, D.J.W. Grant, Influence of elastic deformation of particles on Heckel analysis, Pharmaceutical Development and Technology 6 (2001) 193–200.
[6] R.J. Roberts, R.C. Rowe, The compaction of pharmaceutical and other model materials – a pragmatic approach, Chemical Engineering Science 42 (4) (1987) 903–911.
[7] A. Hassanpour, M. Ghadiri, Distinct element analysis and experimental evaluation of the Heckel analysis of bulk powder compression, Powder Technology 141 (3) (2004) 251.
[8] P.J. Denny, Compaction equations: a comparison of the Heckel and Kawakita equations, Powder Technology 127 (2) (2002) 162–172.
[9] M.J. Adams, R. McKeown, Micromechanical analyses of the pressure–volume relationship for powders under confined uniaxial compression, Powder Technology 88 (2) (1996) 155–163.
[10] B. Johansson et al., Compression behaviour and compactability of microcrystalline cellulose pellets in relationship to their pore structure and mechanical properties, International Journal of Pharmaceutics 117 (1) (1995) 57–73.
[11] M. Wikberg, G. Alderborn, Compression characteristics of granulated materials II. Evaluation of granule fragmentation during compression by tablet permeability and porosity measurements, International Journal of Pharmaceutics 62 (2–3) (1990) 229–241.
[12] M. Duberg, C. Nyström, Studies on direct compression of tablets VI. Evaluation of methods for the estimation of particle fragmentation during compaction, Acta Pharmaceutica 19 (6) (1982) 421–436.
[13] W.C. Duncan-Hewitt, G.C. Weatherly, Modeling the uniaxial compaction of pharmaceutical powders using the mechanical properties of single crystals. II: brittle materials, Journal of Pharmaceutical Sciences 79 (3) (1990) 273–278.
[14] I. Shapiro, Compaction of powders 11. Application of the general equation to both metal powders and ceramic powders, Advances in Powder Metallury and Particulate Materials 3 (1994) 41–55.
[15] J. Nordström et al., A particle rearrangement index based on the Kawakita powder compression equation, Journal of Pharmaceutical Sciences (2008), doi:10.1001/jps.21488.
[16] C. Ahlneck, G. Alderborn, Moisture adsorption and tabletting. I. Effect on volume reduction properties and tablet strength for some crystalline materials, International Journal of Pharmaceutics 54 (2) (1989) 131–141.
[17] B.H. Kaye, Permeability techniques for characterizing fine powders, Powder Technology 1 (1967) 11–22.
[18] F. Nicklasson, G. Alderborn, Compression shear strength and tableting behavior of microcrystalline cellulose agglomerates modulated by a solution binder (polyethylene glycol), Pharmaceutical Research 18 (6) (2001) 873–877.
[19] G. Alderborn et al., Studies on direct compression of tablets X. Measurement of tablet surface area by permeametry, Powder Technology 41 (1) (1985) 49–56.
[20] G. Alderborn, C. Nyström, Studies on direct compression of tablets III. The effect in tablet strength of changes in particle-shape and texture obtained by milling, Acta Pharmaceutica 19 (2) (1982) 147–156.
[21] J. Nordström et al., On the physical interpretation of the Kawakita and Adams parameters derived from confined compression of granular solids, Powder Technology 182 (3) (2008) 424–435.
[22] J.M. Sonnergaard, Impact of particle density and initial volume on mathematical compression models, European Journal of Pharmaceutical Sciences 11 (4) (2000) 307–315.
[23] J. Nordström et al., On the role of granule yield strength for the tableting forming ability of granular solids, J. Pharm. Sci. (2007), doi:10.1002/jps.21351.
[24] G. Alderborn, C. Nyström, Studies on direct compression of tablets XIV. The effect of powder fineness on the relation between tablet permeametry surface area and compaction pressure, Powder Technology 44 (1) (1985) 37–42.
[25] M. Eriksson, G. Alderborn, The effect of original particle size and tablet porosity on the increase in tensile strength during storage of sodium chloride tablets in a dry atmosphere, International Journal of Pharmaceutics 113 (2) (1995) 199–207.
[26] J.M. Sonnergaard, A critical evaluation of the Heckel equation, International Journal of Pharmaceutics 193 (1) (1999) 63–71.
[27] M. Duberg, C. Nyström, Studies on direct compression of tablets XVII. Porosity–pressure curves for the characterization of volume reduction mechanisms in powder compression, Powder Technology 46 (1) (1986) 67–75.
[28] G. Alderborn et al., International Journal of Pharmaceutics 23 (1) (1985) 79–86.
[29] K. Kawakita, K.-H. Ludde, Some considerations on powder compression equations, Powder Technology 4 (2) (1971) 61–68.
[30] R.J. Roberts et al., Brittle–ductile transitions in die compaction of sodium chloride, Chemical Engineering Science 44 (8) (1989) 1647–1651.
[31] P. Paronon, J. Ilkka, Porosity–pressure functions, in: G. Alderborn, C. Nyström (Eds.), Pharmaceutical Powder Compaction Technology, Marcel Dekker, New York, 1996, pp. 55–77.